

A Multi-analytical Non-invasive Approach to Aqueous Cleaning Systems in Treatments on Bowed String Musical Instruments

Ilaria Cazzaniga ^{1,2}, Marco Gargano ^{1,*}, Claudia Invernizzi ^{3,4}, Nicola G. Ludwig ¹, Marco Malagodi ^{3,5}, Claudio Canevari ⁵ and Tommaso Rovetta ³

¹ Department of Physics, Università degli Studi di Milano, via Celoria 16, 20133 Milano, Italy; ilariacazzaniga21@gmail.com (I.C.); nicola.ludwig@unimi.it (N.G.L.)

² Violin Making School of Milan, via Noto 4, 20141 Milan, Italy

³ Arvedi Laboratory of non-Invasive Diagnostics, CISRI-C, University of Pavia, via bell'Aspa 3, 26100 Cremona, Italy; claudia.invernizzi@unipv.it (C.I.); marco.malagodi@unipv.it (M.M.); tommaso.rovetta@unipv.it (T.R.)

⁴ Department of Mathematical, Physical and Computer Sciences, University of Parma, Parco Area delle Scienze 7/A, 43124 Parma, Italy

⁵ Department of Musicology and Cultural Heritage, University of Pavia, Corso Garibaldi, 178, 26100 Cremona, Italy; canevari.c@gmail.com

* Correspondence: marco.gargano@unimi.it; Tel.: +39 0250317472

S1. Multispectral Imaging

S1.1 Data Analysis

The color difference has been evaluated comparing color coordinates (L^* , a^* , b^*) from reference varnished areas left unsoiled on the left border of each mock-ups in two different stages, just after the soiling procedure and after the cleanings (it has been about a month). This change has to be taken into account once we look at the color difference between dirty and cleaned areas. However, the varnish color change might have been different and maybe smaller in the areas where dirt was spread in comparison to the varnish left uncovered by soil. Therefore, an evaluation of the color contribution by varnish change is done, but this evaluation cannot be approached quantitatively in order to correct cleaned areas colors (i.e., subtracting its contribution to color difference between before and after cleaning procedure) or a systematic error would be added.

Varnish changes were evaluated both in visible images and in visible UV-induced fluorescence ones. Color changes are displayed in Figure S1–S4 and relative color differences are presented in Table S1. A trend in color change can be observed: lightness increase in most cases and a shift towards reds (positive values of a^*) and yellows (positive values of b^*) in visible images.

Citation: Cazzaniga, I.; Gargano, M.; Invernizzi, C.; Ludwig, N.G.; Malagodi, M.; Canevari, C.; Rovetta, T. A multi-analytical non-invasive approach to aqueous cleaning systems in treatments on bowed string musical instruments. *Coatings* **2021**, *11*, 150. <https://doi.org/10.3390/coatings11020150>

Received: 28 December 2020

Accepted: 27 January 2021

Published: 29 January 2021

Publisher's Note: MDPI stays neutral with regard to jurisdictional claims in published maps and institutional affiliations.



Copyright: © 2021 by the authors. Submitted for possible open access publication under the terms and conditions of the Creative Commons Attribution (CC BY) license (<http://creativecommons.org/licenses/by/4.0/>).

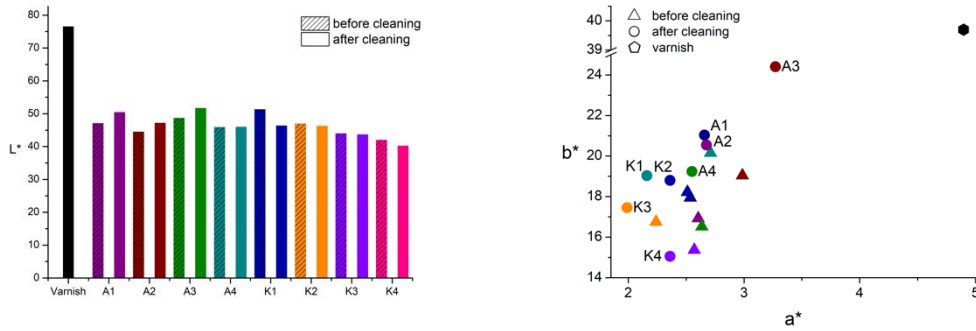


Figure S1. Chromatic coordinates (right graphs) and lightness (left graph) calculated from visible images from varnished reference mock-up (red) and before (blue) and after (yellow) the cleaning performed on mock-up I.

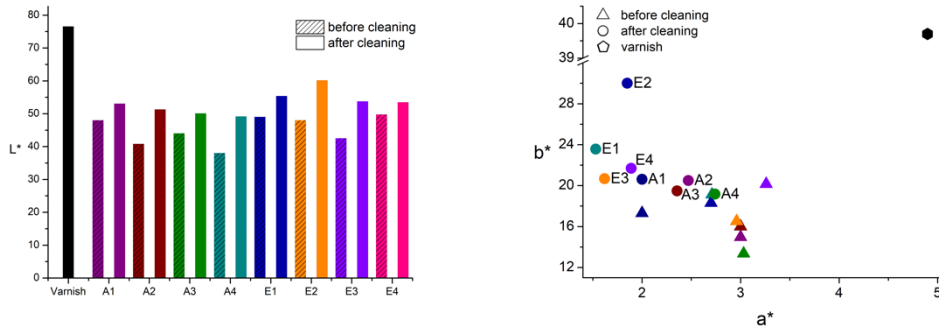


Figure S2. Lightness (left graph) and chromatic coordinates (right graph) calculated from visible images from varnished reference mock-up (red) and before (blue) and after (yellow) the cleaning performed on mock-up II.

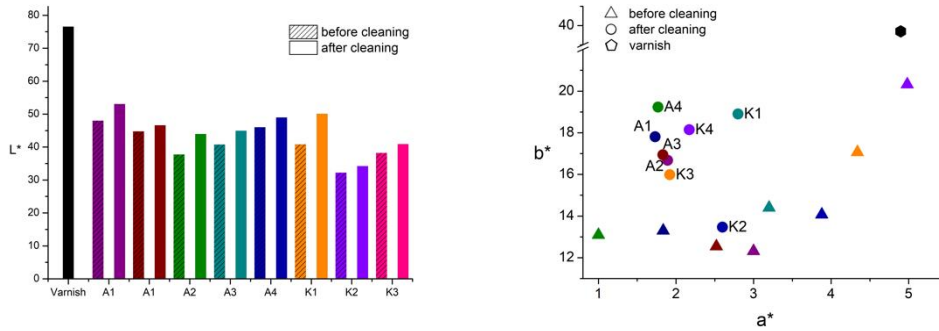


Figure S3. Lightness (left graph) and chromatic coordinates (right graph) calculated from visible images from varnished reference mock-up (red) and before (blue) and after (yellow) the cleaning performed on mock-up III.

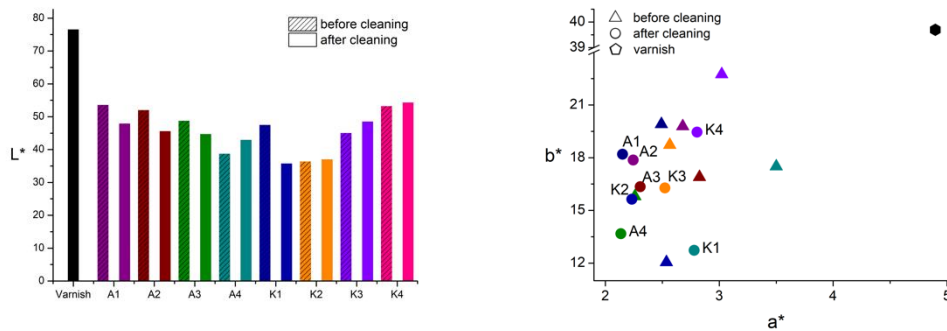


Figure S4. Lightness (left graph) and chromatic coordinates (right graph) calculated from visible images from varnished reference mock-up (red) and before (blue) and after (yellow) the cleaning performed on mock-up IV.

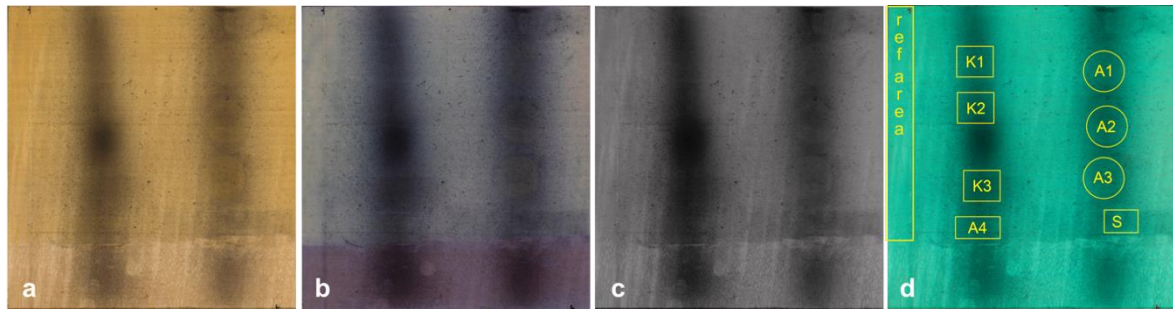


Figure S5. Multispectral imaging of mock-up I: VIS (a), UVIFL (b), NIR (c) and IRFC (d).

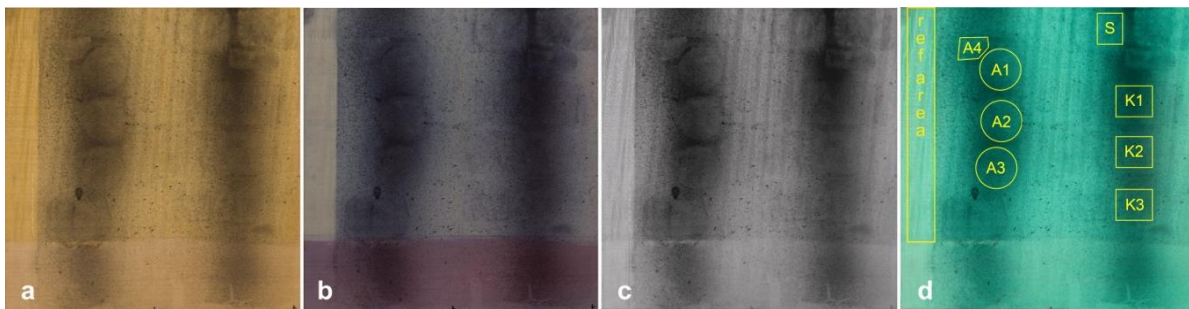


Figure S6. Multispectral imaging of mock-up III: VIS (a), UVIFL (b), NIR (c) and IRFC (d).

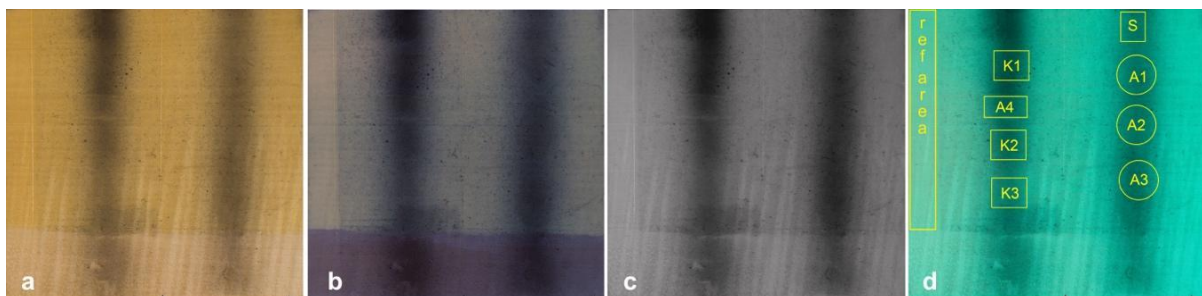


Figure S7. Multispectral imaging of mock-up IV: VIS (a), UVIFL (b), NIR (c) and IRFC (d).

Table S1. Color differences between (L^* , a^* , b^*) values of the same areas of each mock-ups before and after the cleaning treatment.

Mock-up	Cleaning Treatment	ΔL_{00} (+/- 0.01)	ΔC_{00} (+/- 0.3)	ΔH_{00} (+/- 0.3)	ΔE_{00} (+/- 0.3)
I	A1	3.28	1.6	0.4	3.7
	A2	2.61	1.9	0.6	3.3
	A3	2.89	2.8	0.8	4.2
	A4	0.09	1.4	0.6	1.6
	K1	4.82	0.7	0.3	4.9
	K2	1.08	0.3	0.2	1.2
	K3	0.35	0.3	0.3	0.6
	K4	1.45	-0.2	0.1	1.5
II	A1	4.48	1.7	1.2	5.0
	A2	9.69	2.9	1.5	10.3
	A3	5.44	1.8	1.2	5.9
	A4	10.44	3.0	1.7	11.0
	E1	5.90	2.3	1.8	6.6
	E2	11.33	6.4	2.4	13.3
	E3	10.42	2.1	2.1	10.9
	E4	3.46	0.7	1.2	3.8
III	A1	1.69	2.5	0.9	3.2
	A2	5.61	2.3	1.9	6.4
	A3	3.80	2.3	1.7	4.8
	A4	2.63	3.5	0.6	4.5
	K2	1.81	-0.7	1.2	2.3
	K3	2.44	-1.1	2.4	3.5
	K4	1.97	-1.7	2.3	3.4
IV	A1	5.46	1.0	0.0	1.0
	A2	6.16	1.1	0.1	1.1
	A3	3.91	0.4	0.4	0.6
	A4	4.11	1.2	0.3	1.2
	K2	0.61	1.9	1.1	2.3
	K3	3.36	1.3	0.5	1.4
	K4	1.07	1.8	0.5	1.9

S2. EDXRF Spectroscopy

S2.1 Data Analysis

Spectra of dirty surfaces were collected in twenty different spots and the net area count average of each element ($K\alpha$ peak), together with standard deviation and SDOM, were calculated (Table S2). Since the soiling procedure did not produce uniform thicknesses of dirt on the mock-ups and the point of analysis is quite small (1.2 mm²), statistical methods were employed to evaluate cleaning results. In this way we can say with a certain confidence if area counts are changed or not after the cleaning treatment, in respect to the dirty surface area counts.

Standard deviation values represent the spreading of measurements around the real value and were useful to evaluate if changes in counts per area after cleaning is relevant or not: if the cleaned area counts are noticeably fewer (i.e., the “cleaned” value is far more than 1 standard deviation from the “dirty” value), we can affirm that the concentration of that element is lower and a certain amount of it has been removed by the cleaning. On this basis, we can affirm that peaks can be considered statistically relevant. For the same purpose, we observed the trend of results concerning each treatment at different times of application and their consistency. These procedures were adopted since one single measurement per each cleaned area was taken and its variation could not be obtained from data.

Secondly, it must be considered that the concentration of lighter elements ($Z < 11$) could be underestimated with respect to their real amount, because their secondary radiations have low penetrating power and are severely attenuated by the air and any matrix for any distance [4]. For this reason, aluminum and phosphorus peaks were not taken into account since they are too low, and their variations are not valuable with the standard deviation method explained above. On the other hand, Si and S count variations are valuable by comparing measurements of dirty spots and cleaned ones. However, in these cases it is not possible to distinguish differences between one cleaned spot measurement and another to establish cleaning effectiveness.

Table S2. Normalized net area count average and relative SDOM of each emission peak ($K\alpha$) identified in EDXRF spectrum.

Detected Element	Normalized Net Area Counts (average on 7 spots)	Standard Deviation of the Mean (SDOM)
Si	0.16	0.01 (5%)
S	0.040	0.004 (9%)
K	0.44	0.04 (9%)
Ca	5.6	0.4 (7%)
Fe	0.52	0.03 (6%)

S2.2 Heat Maps

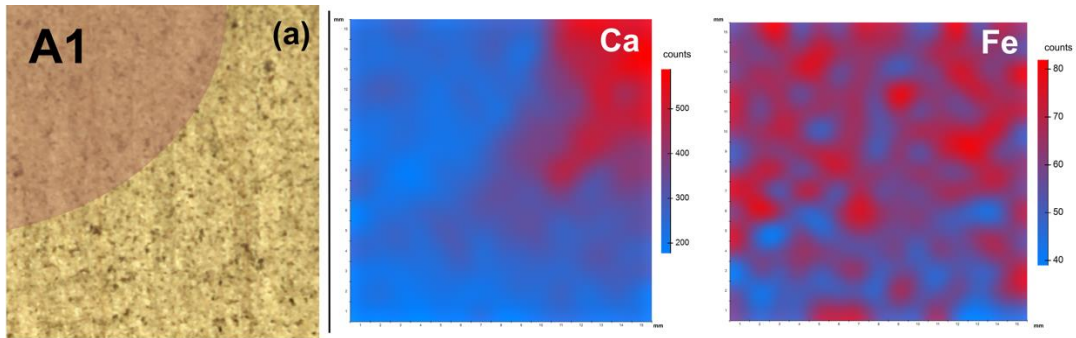


Figure S8. EDXRF heat maps on a selected area of mock-up I. Higher and lower relative concentrations of each characteristic element are presented respectively in red and blue colors. Stitch visible image (a) of the area (15 mm × 15 mm) considered for the XRF mapping.

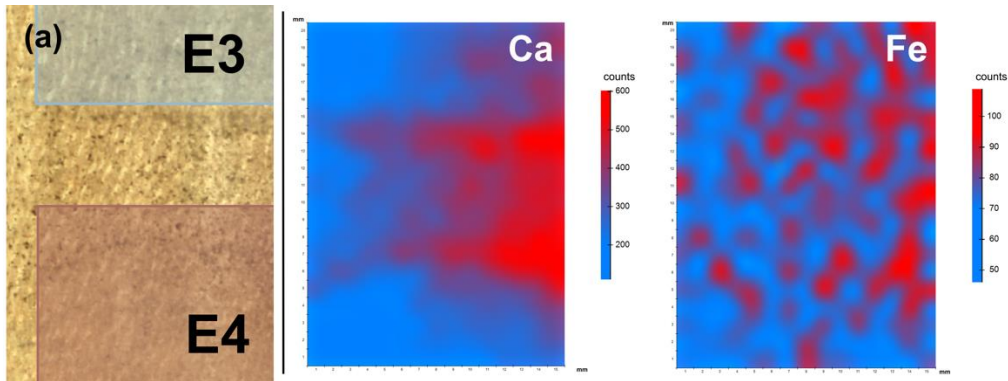


Figure S9. XRF heat maps on a selected area of mock-up II. Higher and lower relative concentrations of each characteristic element are presented respectively in red and blue colors. Stitch visible image (a) of the area (15 mm × 20 mm) considered for the XRF mapping.

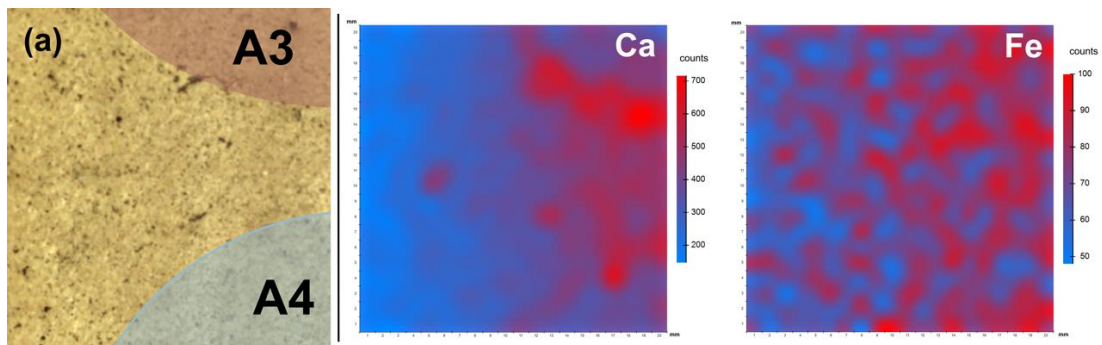


Figure S10. XRF heat maps on a selected area of mock-up IV. Higher and lower relative concentrations of each characteristic element are presented respectively in red and blue colors. Stitch visible image (a) of the area (15 mm × 20 mm) considered for the XRF mapping.

S3. Varnish FTIR Reference Spectra

Table S3. Reflection FTIR wavenumber values, and their assignment [5,6], of the bands identified in dried oil-colophony varnished mock-ups.

Wavenumber	Band Shape	Assignment	Material Attribution
2955 (w)	Derivative	$\nu_{as}CH_2$	Colophony
2927 (s)	Derivative	$\nu_{as}CH_2$	Linseed oil
2854 (s)	Derivative	ν_sCH_2	Linseed oil
1735 (s)	Derivative	$\nu C-O$	Linseed oil
1459 (m)	Derivative	in-plane δ_sCH_2	Colophony, linseed oil
1383 (w)	Derivative	δ_sCH_3	Colophony
1165 (m)	Derivative	$\nu C-O$	Linseed oil
1087 (s)	Derivative	$\nu_{as}Si-O$	Diatomaceous earth
792 (m)	Inverted	vs $Si-O-Si$, $Si-O-Al$, $(Si,Al)-O-(Si,Al)$	Diatomaceous earth
613 (w)	Inverted	$\delta Si-O$	Diatomaceous earth
477 (s)	Inverted	$\delta Si-O$	Diatomaceous earth

References

1. Madejová, J.; Komadel, P. Baseline studies of the clay minerals society source clays: infrared methods. *Clays Clay Miner.* **2001**, *49*, 410–432.
2. Miller, F.A.; Wilkins, C.H. Infrared spectra and characteristic frequencies of inorganic ions. *Anal. Chem.* **1952**, *24*, 1253–1294.
3. Yang, H.; Yan, R.; Chen, H.; Lee, D.H.; Zheng, C. Characteristics of hemicellulose, cellulose and lignin pyrolysis. *Fuel* **2007**, *86*, 1781–1788.
4. Glinsman, L.D. The practical application of air-path X-ray fluorescence spectrometry in the analysis of museum objects. *Stud. Conserv.* **2005**, *50*, 3–17, doi:10.1179/sic.2005.50.Supplement-1.3.
5. Invernizzi, C.; Daveri, A.; Vagnini, M.; Malagodi, M. Non-invasive identification of organic materials in historical stringed musical instruments by reflection infrared spectroscopy: a methodological approach. *Anal. Bioanal. Chem.* **2017**, *409*, 3281–3288, doi:10.1007/s00216-017-0296-8.
6. Invernizzi, C.; Fichera, G.V.; Licchelli, M.; Malagodi, M. A non-invasive stratigraphic study by reflection FT-IR spectroscopy and UV-induced fluorescence technique: The case of historical violins. *Microchem. J.* **2018**, *138*, 273–281, doi:10.1016/j.microc.2018.01.021.